JOURNAL OF CATALYSIS 137, 77–91 (1992)

Supported Ru–Mo Catalysts for Syngas Reaction to Oxygenates

A. JUAN* AND D. E. DAMIANI†,[1]

Departamento de Física, Universidad Nacional del Sur, 8000 Bahía Blanca, Argentina; and †PLAPIQUI (UNS-CONICET), 12 de Octubre 1842, 800 Bahía Blanca, Argentina

Received July 10, 1991; revised April 6, 1992

Despite numerous reports on the activity and selectivity of modified Ru catalysts on the synthesis of oxygenates from syngas, not many papers have appeared on their characterization. The goal of the research here reported is to provide more information regarding these catalysts. Temperature programmed reduction (TPR), temperature programmed desorption (TPD), temperature programmed surface reaction (TPSR), X-ray diffraction (XRD), and X-ray photoelectron spectroscopy (XPS) results, H_2 and CO chemisorption uptakes, as well as activity and selectivity for the CO + H_2 reaction and Cl^- evolution studies on RuMo catalysts are given here. The catalysts, prepared by co-impregnation of SiO_2 with $RuCl_3 \cdot 1 \cdot 5H_2O$ and $(NH_4)_6Mo_7O_{24} \cdot 4H_2O$, were pretreated according to two different procedures: (I) oxidation at 673 K followed by reduction at 673 K or (II) reduction at 673 K. Pretreatment II eliminates all residual Cl^-. Pretreatment I on the other hand results in higher final Cl^- contents in the catalysts and renders them more selective to oxygenates. The results are interpreted in terms of the existence of Ru–Mo contacts which are necessary for ethanol production and Cl^--containing Ru sites responsible for methanol production.

INTRODUCTION

The selective production of C_2^+ alcohols from CO and H_2 is a subject of not only academic but also commercial interest, due to the continuing decay of oil reserves and the possibility of using natural gas or coal as a source of synthesis gas.

Alcohol mixtures can be used as gasoline additives to increase the octane number. Other important aspects related to superior alcohols are that they can be easily converted to their corresponding olefins, used as solvents or as raw materials in plastics, detergents, and lubricants manufacture. The use of methanol as a gasoline additive introduces the problem of its solubility in hydrocarbons. This can be avoided using alcohol mixtures.

While methanol synthesis is a well established process, the direct synthesis of C_2^+ alcohols is at present in the research and development stage.

Several papers related to catalysts for oxygenate synthesis have appeared (*1, 2*). In many cases production of alcohol mixtures using modified methanol synthesis catalyst has been reported (*3*).

Ruthenium is known for its ability to hydrogenate CO to methane at low pressure and to polymethylenes at high pressure (*4*). Kellner and Bell (*5*) reported in 1981 that, under appropriate conditions, Ru/SiO_2 catalyzes the production of acetaldehyde from CO and H_2, while on Ru/Al_2O_3 the main product observed was methanol. Working on Ru/Al_2O_3 and Ru/MgO at 5.0 MPa and 530 K, Bossi *et al.* (*6*) found what they called a notorious amount of oxygenates as alcohols. They attributed this activity to the presence of $Ru^{\delta+}$ sites. Modification of Ru selectivity toward oxygenates, mainly to methanol after a high temperature treatment in an H_2–H_2O mixture, was reported by Kobori *et al.* (*7*). There are also many reports on the modification of the Ru selectivity to produce oxygenates by the incorporation of a second metal on the catalyst formulation

[1] To whom correspondence should be sent.

0021-9517/92 $5.00

(*8, 9*). Hamada and co-workers (*10*) found good selectivity to C_2 oxygenates on bimetallic Ir–Ru/SiO_2 catalysts prepared from metal chlorides and promoted by alkaline elements. Similarly Inoue *et al.* (*11*) reported that supported Ru–Mo–Na_2O catalysts were able to produce selectively linear alcohols from CO and H_2 at 8.7 MPa and 500 K.

The same authors extended their work on modified Ru catalysts and found that the Ru–Mo contact was necessary in order to have good oxygenate selectivity (*12*). According to them, this Ru–Mo interaction was produced by an adequate Ru precursor. In that sense, $RuCl_3$ was found to be the best. The same research group recently reported the influence of the support acidity and porous structure on the activity and selectivity (*13*).

Despite the numerous reports on the activity and selectivity of modified Ru catalysts, the studies devoted to their characterization are scarce. The goal of the research reported here is to provide more information regarding these catalysts.

In the present paper we report the result of a study we conducted on a set of SiO_2-supported RuMo catalysts using temperature programmed techniques, H_2 and CO chemisorption, Cl^- elimination measurements, XRD and XPS analysis, as well as activity and selectivity determination. The information collected by those means together with that on the catalyst impregnation procedure and thermodynamic data allowed us to develop a model of the catalyst structure after each pretreatment. We speculate on the relationship between such structure and the activity and selectivity of the catalyst in the syngas reaction.

EXPERIMENTAL

Catalyst Preparation

The monometallic Ru and Mo and the bimetallic Ru–Mo catalysts were prepared by co-impregnation of the supports with $RuCl_3 \cdot 1.5H_2O$ (Alfa Ventron Co) and $(NH_4)_6Mo_7O_{24} \cdot 4H_2O$ (BOH Chemical, Ltd., England) using the incipient wetness method.

The support used was SiO_2 Cab-O-Sil M5, Cabot Co., Degussa, Inc., with BET area of 200 m^2/g. The Ru loading was 2 wt%. Molybdenum composition was 50% in atoms. Monometallic catalysts were prepared having the same metal loading as the corresponding metal in the bimetallic sample. The metal content was determined by Atomic Absorption Spectroscopy and it was found to be within ±5% of the nominal value. After impregnation the catalysts were dried in air at room temperature and stored until the experiments were performed. Prior to each type of experiment, the catalysts were subjected to the pretreatment that is indicated below for each case. Basically, it consisted in an oxidation step followed by a reduction step or in a reduction only. The first one is designated as I, the second one as II. Minor changes in the pretreatment were necessary to be introduced in each type of experiment due to the intrinsic nature of the experiment of interest. The following convention is adopted to name the catalysts: 0 RuMo/SiO_2, 50 RuMo/SiO_2, and 100 RuMo/SiO_2 identify the pure Mo, the bimetallic, and the pure Ru catalysts, respectively.

In order to identify which effects were due to chlorine, a pure Ru catalyst was prepared from $Ru(NO)(NO_3)_3 \cdot H_2O$ (Alfa Products) by incipient wetness impregnation of Davison Silica Grade 923 (650 m^2/g). After preparation, the catalyst was dried in air at room temperature for 2 days followed by an additional 2.5 h at 393 K.

Temperature Programmed Reduction (TPR)

TPR experiments were carried out in an apparatus similar to that described by Robertson *et al.* (*14*), to which some modifications were introduced (*15*). The reducing gas was a mixture of 5% H_2 in Ar flowing at 20 cc/min. Temperature was increased at a rate of 8 K/min between 273 and 823 K.

Fresh samples (40 mg) were pretreated ac-

cording to the treatments cited above which in this case were performed as follows: (I′) 1 h oxidation in flowing air at 673 K, followed by another period of 1 h at 373 K, and finally the TPR; (II′) 1 h reduction in flowing H_2 at 673 K, followed by 1 h oxidation in flowing air at 373 K, and the TPR.

Temperature Programmed Desorption (TPD)

Temperature programmed desorption of CO was carried out in the TPR apparatus. Samples treated according to either pretreatment I or II were purged at high temperature in Ar for a period of time. Following that purge, they were cooled in flowing Ar to room temperature and saturated with CO. After the weakly adsorbed CO was removed, the TPD experiment was started. Experimental conditions were chosen following criteria of Gorte (*16*) and Rieck and Bell (*17*), to minimize mass-transfer effects.

Temperature Programmed Surface Reaction (TPSR)

TPSR experiments were performed in a manner similar to the TPD experiments, but using a 10% H_2, 90% Ar stream rather than pure Ar in the programmed heating step. The effluent gases, CH_4, CO_2, and CO, were chromatographically analyzed.

Hydrogen and CO Chemisorption

Hydrogen and CO chemisorption runs were carried out in a conventional volumetric apparatus.

Prior to chemisorption experiments, the catalysts were treated in the adsorption system as follows: (I) oxidation in O_2 at 673 K for 1 h followed by a reduction in H_2 at 673 K for 1 h and an evacuation period of 2 h at the same temperature or (II) reduction in H_2 at 673 K for 1 h followed by evacuation at 673 K for 2 h.

Chemisorption experiments were done at room temperature in the pressure range of 0–200 Torr measured with an absolute pressure gauge provided by MKS Instruments. The equilibration time was 1 h for the first point, 45 min for the second one, and 30 min for subsequent points.

Particle size was calculated assuming a spherical particle having a metal atom surface area of 0.0817 nm^2/atom (*18*).

Water Electrical Conductivity Test

The evolution of gases during treatments I and II was followed by measuring the electrical conductivity of water where the gases were bubbled.

Fresh samples of SiO_2 or supported catalyst were placed in a U-shaped pyrex tube which was heated from 218 to 723 K at a rate of 8 K/min in an electrically heated oven under flowing H_2 (treatment II) or O_2 and then H_2 (treatment I). The effluent gases were bubbled in a 70-ml vase containing bidistilled dechlorinated water whose conductivity was measured by means of a conductivity electrode. In the case of treatment I, the water of the conductivity cell was changed after the O_2 treatment so the reduction step was initiated with a fresh volume of distilled and dechlorinated water.

After the tests, the water was examined for the presence of Cl^- by addition of $AgNO_3$. The remaining catalyst was also examined for the presence of residual Cl^- by boiling it in bidistilled water and testing the filtrate for Cl^- in the same way as before.

The evolution of NH_3 was followed by adding $Cu(NO_3)_2$ and looking for the formation of the blue $[Cu(NH_3)_4]^{2+}$ complex.

X-ray Diffraction

XRD data were obtained using the powder method in a Rigaku diffractometer operated at 36 kV with an Ni filter for the CuKα radiation.

The diffraction patterns were obtained using fresh catalysts or samples slowly passivated in air after pretreatment I or II. Particle size was calculated by X-ray line broadening using the Scherrer equation.

UV Spectroscopy

Ru and Mo solutions with concentrations similar to those of the impregnating solu-

tions were analyzed using this technique in the range 190 to 900 nm.

TEM and SEM

A JEOL 100 Cx electron microscope was used to determine metal particle size. Surface morphology was studied by SEM in a JEOL JSM 35CF.

CO + H_2 Reaction

Activity tests in the CO + H_2 reaction were carried out in a microcatalytic flow reactor made of stainless-steel tubing (6-mm O.D.). The reactor temperature was maintained constant by a controlled electric furnace.

Lines downstream from the reactor, including the backpressure regulator and the sampling valve, were heated in order to prevent condensation. The flow rate was controlled by means of a Matheson mass flow controller. The system was operated at 2 MPa with a CO : H_2 ratio in the feed of 1 : 5 and about 100 mg of catalyst. Reactor effluent gases were chromatographically analyzed using a 3700 Varian Gas-Chromatograph operating in the thermal conductivity mode equipped with two columns in series (Chromosorb 102 and Porapak Q). Hydrogen was used as carrier gas and column temperature was kept constant at 423 K.

Prior to reaction, the catalyst samples were pretreated according to the two different procedures already mentioned, that in this case were performed as follows: (I) oxidation in O_2 at 673 K for 1 h followed by another 1-h period of reduction in H_2 at 673 K or (II) H_2 reduction at 673 K for 1 h, cooling down to room temperature in H_2, admission of the reacting mixture at room temperature and atmospheric pressure, increase pressure to 2 MPa, and heating the reactor to the working temperature.

Ethane Hydrogenolysis

Ethane hydrogenolysis was carried out in a microcatalytic pulse reactor operated at low conversions. Outlet gases were chromatographically analyzed.

TABLE 1

Hydrogen and CO Chemisorption[a]

Catalyst	H/Me_t		CO/Me_t	
	Pretreatment		Pretreatment	
	I[b]	II[b]	I[b]	II[b]
100 RuMo	0.08	0.15	0.03	0.20
50 RuMo	0.01	0.06	0.01	0.04
0 RuMo	0.00	0.02	0.03	0.02

[a] Results reported as H or CO to total metal atoms ratios.

[b] Described in the experimental section for chemisorption experiments.

Gases

Matheson CO (Matheson grade) and AGA special grade H_2 (O_2 = 10 ppm, H_2O = 10 ppm) were used in the preparation of the reaction mixture.

The hydrogen utilized in chemisorption was previously purified by passing it through a heated Pd thimble. UHP O_2 and dried synthetic air were used in catalyst pretreatment.

RESULTS

H_2 and CO Chemisorption

Hydrogen and CO chemisorption experiments on catalysts subject to either treatment I or II gave similar results in the sense that in both cases the presence of Mo produces an important decrease in both gases uptake (see Table 1). The addition of Mo or V to Ru/Al_2O_3 catalyst produced this effect on H_2 adsorption as described by Mori and co-workers (*19*). Kip *et al.* (*20*), Bhore *et al.* (*21*), and Mills (*22*) reported important changes in H_2 and CO adsorption when Rh is deposited on SiO_2 previously impregnated with $(NH_4)_6Mo_7O_{24} \cdot 4H_2O$. On the other hand Hicks *et al.* (*23*) found similar results on Pd/La_2O_3. They postulated that Pd chemisorption ability was modified by the presence of LaOx patches transferred to the Pd surface during the catalyst preparation stages.

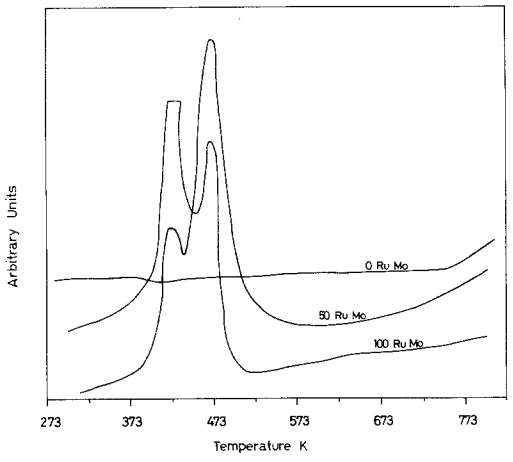

FIG. 1. TPR Profiles of RuMo/SiO_2 after pretreatment I'(O_2, 673 K, 1 h + O_2, 373 K, 1 h).

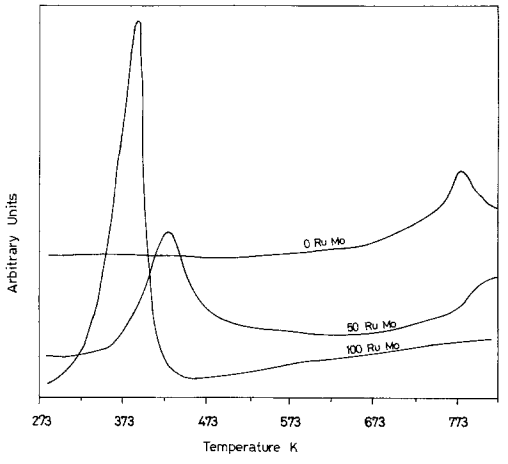

FIG. 2. TPR Profiles of RuMo/SiO_2 after pretreatment II' (H_2, 673 K, 1 h + O_2, 373 K, 1 h).

In our case, the change in H_2 uptake between the pure Ru and the bimetallic is more important in the catalysts treated according to procedure II.

The pure Mo catalyst shows little H_2 and CO uptake after treatment II, therefore part of the hydrogen consumed in the adsorption experiment on the bimetallic treated similarly must be attributed to the reduction of the Mo precursor. On the other hand, H_2 chemisorption was suppressed on Mo/SiO_2 treated according to I.

Temperature Programmed Reduction

Temperature programmed profiles are shown in Figs. 1 and 2. It can be seen that Mo reduction begins at approximately 723 K. Hydrogen consumption about six times higher for the Mo catalyst treated according to pretreatment II, as shown in Table 2. It is known that after being exposed to hydrogen at 773 K, Mo is more easily reduced when supported on SiO_2 than on the other supports (*24*). Reduction profiles similar to ours were obtained by Kip *et al.* (*20*) for Mo/SiO_2 catalysts calcined at 723 K. They attributed it to the $Mo^{6+} \rightarrow Mo^{+4}$ reduction.

Comparing the TPR profiles of catalysts subject to pretreatment II, it is possible to observe a shift to higher temperatures of the Ru reduction peak while hydrogen consumption is 40% lower than in the case of pure Ru catalyst. This observation indicates an Ru–Mo interaction, and it is consistent with H_2 chemisorption results that show a drop of the H to metal atom ratio from 0.15 to 0.06 when Mo is incorporated in the catalyst. Similar results have been previously reported by several authors (*22, 25–28*).

For those catalysts treated according to procedure I in the TPR experiments, there is evidence that less Mo is being reduced

TABLE 2

Relative Areas under the H_2 Consumption Peak in the TPR Profiles[a]

Catalysts	Reduction of	Pretreatment[b]	
		I'	II'
100 RuMo	Ru	1	0.87
50 RuMo	Ru	0.96	0.52
	Mo	0.10	0.15
0 RuMo	Mo	0.05	0.33

[a] H_2 consumption was estimated as the area under the TPR profiles up to the end of the experiment (823 K) referred to the consumption of H_2 in the TPR of 100 RuMo after pretreatment I'.

[b] I': O_2, 673 K, 1 h; O_2; 373 K, 1 h. II': H_2, 673 K, 1 h; O_2; 373 K, 1 h.

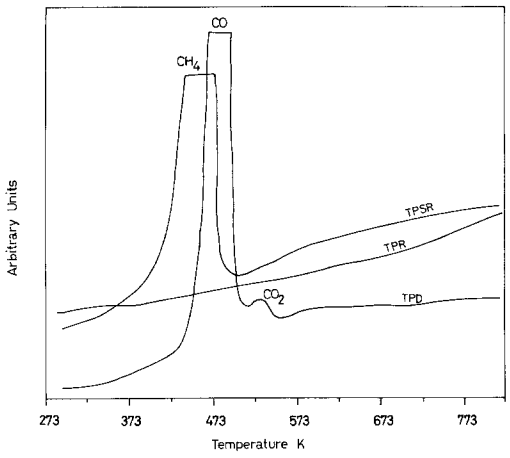

FIG. 3. Profiles of TPR and TPD of CO, and TPSR of CO preadsorbed at room temperature corresponding to 100 RuMo/SiO_2, pretreatment II (H_2, 673 K, 1 h).

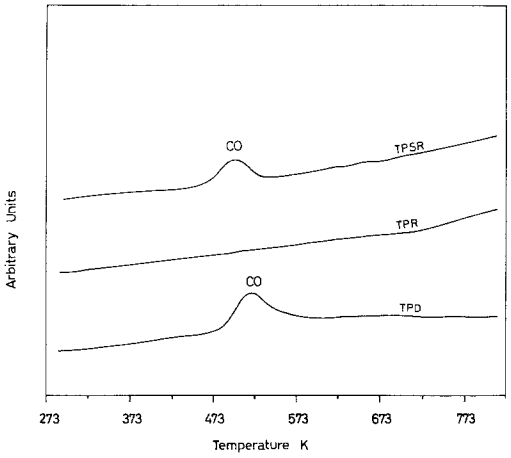

FIG. 4. Profiles of TPR and TPD of CO, and TPSR of CO preadsorbed at room temperature corresponding to 0 RuMo/SiO_2, pretreatment II (H_2, 673 K, 1 h).

during the TPR, not only in the bimetallic samples but also in the pure Mo one. The double peak observed in the TPR profile of pure Ru exposed to pretreatment I can be attributed to the existence of a bimodal particle size distribution. If this were the case, the peak at the higher temperature could be assigned to the reduction of the smaller particles, which, due to its size, could be completely oxidized. The first peak should be originated in the reduction of larger particles, that are partially oxidized and maintain some Ru atoms where hydrogen dissociates and reduction initiates.

Temperature Programmed Desorption and Temperature Programmed Surface Reaction

The results of these experiments are shown in Figs. 3 to 6. For 100 RuMo (pure Ru) exposed to treatment II, the TPD profile of pre-adsorbed CO presents CO and CO_2 peaks at 473 and 530 K, respectively, while only CH_4 is observed in the TPSR profile. CO dissociates at lower temperature in the presence of H_2. This was previously observed in our laboratory (*29*). CO preadsorbed on pure Mo catalyst exposed to treatment II desorbs during the TPD experiment. This result is consistent with the fact that H_2 and CO chemisorption was also observed on this catalyst after similar treatment. Miura *et al.* (*30*) working on catalysts prepared from $H_9PMo_{12}O_{40} \cdot xH_2O$ observed that on previously reduced samples, CO desorbed at lower temperatures. The explanation is related to the weaker CO–Mo bonding compared to that on other noble metals.

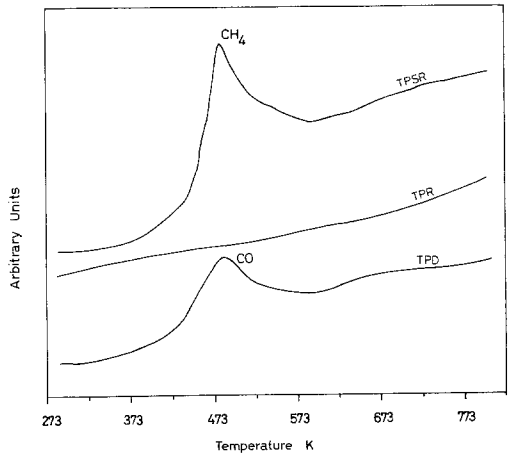

FIG. 5. Profiles of TPR and TPD of CO, and TPSR of CO preadsorbed at room temperature corresponding to 50 RuMo/SiO_2, pretreatment II (H_2, 673 K, 1 h).

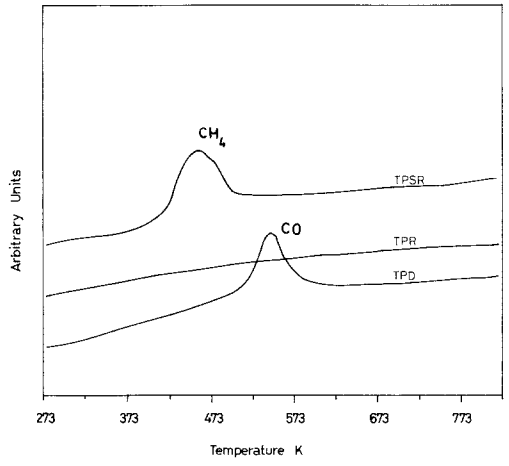

FIG. 6. Profiles of TPR and TPD of CO, and TPSR of CO preadsorbed at room temperature corresponding to 100 RuMo/SiO_2, pretreatment I (O_2, 673 K, 1 h + H_2, 673 K, 1 h).

In the case of the bimetallic catalyst treated according to II, no temperature difference is observed between the CO and CH_4 peaks. The most relevant fact is the relatively small amount of gases desorbed.

For catalyst pretreated following procedure I, the TPD profiles are indicative that the main portion of the pure adsorbed gas is removed from the catalyst surface during the purging step prior to the initiation of the experiment. Chemisorption results on these catalysts are helpful in understanding this result.

Chlorine Monitoring

Additional information was obtained by water conductivity measurements.

Samples of 100 RuMo and 50 RuMo were treated according to procedures I and II with simultaneous monitoring of the conductivity of the water where the effluent gases were bubbled through.

For these catalysts the conductivity of the water in the case of treatment II increases much more than its counterpart for treatment I, meaning that Cl removal was more efficient in the first case. Besides, the change in the water conductivity during the oxidation step of treatment I did not continue during the reduction step (see Fig. 7). Since the initial content of chlorine of the catalyst is the same, it is clear then, that after treatment I part of the initial chlorine is still in the catalyst. In order to verify this, pretreated catalyst samples were boiled in water and after filtering the solid the solution was tested for the presence of Cl^- by adding silver nitrate. The solution corresponding to the sample pretreated according to II remained clear. The other turned turbid, due to the precipitation of AgCl. It is obvious then that after pretreatment I, residues of the precursors are still in the catalyst. These observations are consistent with those reported by Bond *et al.*, Koopman *et al.*, Bossi *et al.*, Blanchard *et al.*, and Mieth and Schwarz (*31–35*).

The water where the effluent gases were bubbled during the treatments was also tested for the presence of Cl^- by adding silver nitrate. In the case of catalysts pretreated following procedure II, the test revealed the existence of Cl^-, while it was negative in the case of the sample treated according to I. The latter was taken as an indication that the change in the water conductivity during the oxidation step is not due to the presence of Cl^- but probably to ClO_y^{-n}. As previously stated, the reduction

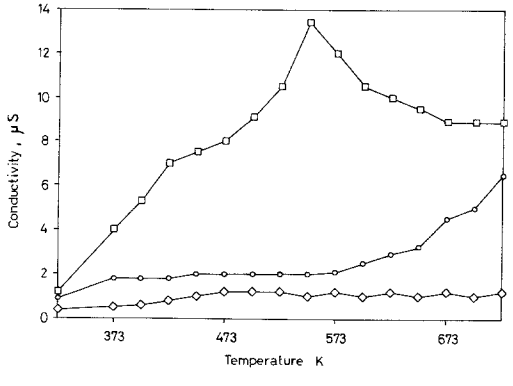

FIG. 7. Chlorine evolution during the pretreatment of 100 RuMO/SiO_2: (○) oxidation step of pretreatment I; (◇) reduction after oxidation step in pretreatment I; (□) pretreatment II.

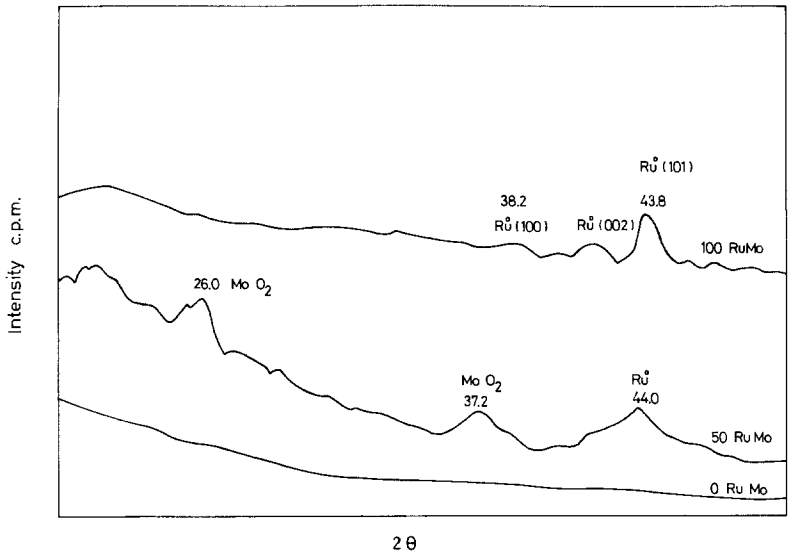

FIG. 8. XRD patterns of 0, 50, and 100 RuMo/SiO_2, pretreatment I (O_2, 673 K, 1 h + H_2, 673 K, 1 h).

step that followed the oxidation, did not alter significantly the conductivity of the water and the test for Cl^- was also negative.

Finally, no NH_3 evolution was detected during the treatments of the bimetallic samples. It is possible then that the Mo precursor decomposes with evolution of N_2.

It is worth mentioning that these tests were also conducted on catalysts pretreated according to treatment I discharged from the reactor after several hours of exposure to the CO hydrogenation reaction. The test revealed the presence of Cl^- in the catalysts even after reaction.

X-Ray Diffraction

For those catalysts treated according to procedure I, an Ru sintering is observed, not only for 100 RuMo but also for the bimetallic. The XRD pattern of 50 RuMo (Fig. 8) has reflections at 2θ, 26°, 37°, and 53°, that may be attributed to MoO_2.

In the case of 100 RuMo after treatment II, no signal is detected indicative of the presence of Ru crystallites. Similarly, no Mo signal is evident in the patterns of the monometallic Mo catalysts. This is taken as an indication of the existence on the surface of an amorphous Mo compound. There are previous reports of similar observations on low Mo loading SiO_2-supported catalysts (*36*).

Samples of newly impregnated catalysts were analyzed by XRD. In all cases, the result was the pattern of amorphous SiO_2.

Particle sizes were calculated using the Scherrer equation. Results are summarized in Table 3 where particle diameters estimated from hydrogen chemisorption data are also given. The latter are larger than those calculated from XRD data, particularly for 50 RuMo after treatment I.

TABLE 3

Metal Particle Sizes Obtained from X-ray Line Broadening and H_2 Chemisorption Data

Catalyst pretreatment:	Average particle diameter (Angstroms)	
	XRD	H_2 chemisorption
100 RuMo (I)	92.7	148.7
100 RuMo (II)	nd	79.3
50 RuMo (I)	130.4	1089.3
50 RuMo (II)	nd	198.2

TABLE 4

CO Hydrogenation on Ru–Mo Catalysts Subjected to Pretreatment I or II

Catalyst	Treatment	CO conversion (%)	Selectivity[a]							
			C_1	C_2	$C_2^=$	C_3	$C_3^=$	MeOH	E_tOH	CO_2
100 RuMo	I	11	40	12	7	13	15	11	—	3
50 RuMo		5	35	19	—	11	—	13	4	18
0 RuMo		1	—	27	12	16	10	16	—	19
100 RuMo	II	99	99	—	—	—	—	—	—	—
50 RuMo		96	90	3	—	—	—	1	2	2
0 RuMo		12	6	—	27	15	10	15	—	27

Note. Described in the Experimental section for CO + H_2 reaction experiments. Data taken after 1 h of reaction. Reaction conditions: 553 K; 2.02 MPa; 20 cm^3/min; $H_2:CO = 5:1$. Results expressed on a water-free basis.

[a] Selectivity is defined as: $iMi/\sum_i Mi$ where M_i is moles of product i and i is the number of carbon atoms in that product.

UV Spectroscopy

The UV spectroscopy spectra of the precursors solution used in the impregnation procedure indicate the lack of interaction between Ru and Mo ions in solution, since the spectrum of the bimetallic solution is the sum of the individual spectra of each metal precursor solution.

Transmission Electron Microscopy

Our TEM results only confirmed the existence of metallic particles bigger than 100 Å in 100 RuMo after treatment I.

CO Hydrogenation Activity Tests

The results of the activity tests, which were made at the same temperature and with equal masses of catalysts, are shown in Table 4. It can be observed that they are a function of the metal composition as well as the pretreatment. Catalysts pretreated according to procedure II are more active than those subjected to pretreatment I. However, the latter have a better selectivity to oxygenates, mainly methanol and ethanol, although the comparison is made at different conversions.

For pretreatment I, in general, the most favorable metal composition in terms of oxygenate product distribution is 50 RuMo. For 100 RuMo, the reaction product is a mixture of hydrocarbons, methanol, and CO_2, while 0 RuMo is almost inactive. Methanol is the most abundant oxygenate on those SiO_2-supported catalysts that showed activity.

For the series pretreated according to procedure II prior to reaction experiments, the results show that methane is the most abundant product while methanol and ethanol are the main oxygenate products and they are observed when Mo is present in the catalyst.

Catalysts to which pretreatment I was applied are less active than their counterparts pretreated with routine II, but they show higher selectivity to oxygenates, mainly methanol and ethanol. 100 RuMo pretreated with procedure I is the only case in which pure Ru showed activity for oxygenate production. Similar observations were made by Kobori *et al.* (*7*), are already mentioned in the Introduction.

DISCUSSION

The goal of this research was to study a series of Ru catalysts and to correlate their

activity and selectivity for the syngas reaction with the result of two different pretreatments and the addition of Mo as a second metal.

The results of H_2 and CO chemisorption show that there is a decrease in both gases uptake after treatment I and upon addition of Mo. Let us first discuss the case of pure Ru catalysts. In this case, the decrease may recognize different causes:

(i) Ru particle sintering.

(ii) Part of the precursor remains on the surface preventing H_2 (as well as CO) access to it.

(iii) The reduction step in treatment I is not enough to completely reduce the particles previously oxidized.

When considering the first cause, it is interesting to keep in mind that the molar volumes of $RuCl_3$ and RuO_2 are 60–80 cm^3/mol and 20 cm^3/mol, respectively. As a consequence of that, Ru atom nucleation is more difficult using treatment II, while pretreatment I leads to larger Ru particles. This is evident in the XRD analysis (see Fig. 8). The XRD analysis of catalyst subjected to treatment II gave no indication of the presence of Ru regardless that H_2 chemisorption indicates that Ru particles are larger than 30 Å. This could be attributed to an amorphous metallic phase on the surface. Ruthenium trichloride deposited on a glass plate gave no indication of crystalline structure. On the other hand, the XRD pattern of fresh catalysts oxidized at 673 K corresponds to that of RuO_2, with peaks at 2°, 28°, and 35°. Catalysts reduced at 873 K for 2 h in a 10% H_2 in Ar stream were slightly sintered as evidenced by the small XRD signal at 2θ = 43°. Therefore, even the exposure to more severe reduction conditions does not result in the sintering observed after the oxidation step. The differences then between pretreatments is the formation of an intermediate crystalline oxide in one of them, which favors the final crystalline state of Ru after treatment I.

The dechlorination studies indicate that part of the chlorine added to the catalyst with the metal precursor remains in it after pretreatment I. The chlorine liberated was not detected as Cl^-. Therefore, the increase in the conductivity of the solution where the treatment gases leaving the catalyst were bubbled is attributed to ClO_x^{-n} species.

It is known that the presence of chlorine and an incomplete reduction strongly affect H_2 and CO chemisorption (*37–39*). Davidov and Bell (*40*) conducted infrared studies on the CO adsorption on oxidized Ru/SiO_2 prepared from chlorides. They found an increment of the CO frequency that moved towards that corresponding to Ru compounds containing CO and Cl ($Ru(CO)_xCl_x$). It is postulated that the elimination of a chloride ion leaves an empty surface site that can be occupied by an additional CO or H_2 molecule. This suggests that Cl^- is bonded to a metallic site rather than to the support, particularly in the case of SiO_2, which does not retain significant amounts of Cl^- (*41–43*). Lu and Tatarchuk found that H_2 adsorption is strongly activated on Ru/Al_2O_3 catalysts prepared from $RuCl_3$, while this is not the case for catalysts prepared from $Ru_3(CO)_{12}$. These observations suggest the presence of electronegative atoms adsorbed on Ru (*43*). Regarding the existence of chlorine during CO hydrogenation, Stoop *et al.* (*44*) reported the presence of HCl in the reactor effluent when using Ru/SiO_2, revealing that complete Cl elimination is not achieved as our results demonstrate.

Regarding cause (iii) it is interesting to keep in mind the process that lead to the metallic phase:

$$\text{(A)}\quad RuCl_3(s) + O_2(g) \rightarrow RuO_2(s) + 4\,Cl_yO_x$$

$$RuO_2(s) + 2H_2(g) \rightarrow Ru(s) + 2H_2O$$

$$\text{(B)}\quad RuCl_3(s) + H_2(g) \rightarrow Ru(s) + x\,HCl(g).$$

Under reduction conditions normally used in the experiments, the equilibrium ratios of $RuCl_3$ are five orders of magnitude higher than those of the oxide. Therefore, chloride reduction is easier than oxide reduction (*45*). According to this, although the

Ru compound on the surface might be a mixture of different Ru chlorides, incomplete reduction is possible after treatment I.

It is time now to look at the relationship between percentage metal exposed obtained from H_2 chemisorption assuming that one Ru surface atom adsorbs one H atom, and the particle sizes determined from XRD data.

Table 3 shows that for O_2-treated 100 RuMo, the average particle diameter obtained by XRD is smaller than that calculated using chemisorption information. Keeping in mind that the first technique cannot detect small crystallites while the second one only detects surface metal atoms, our results lead us to conclude that the adsorption sites are blocked by Cl remaining in the catalysts exposed to an oxidation treatment.

For catalysts prepared from Ru nitrosylnitrate, the mean particle size measured by XRD after treatments I and II is 246.1 and 300.8 Å, respectively. On the other hand, particle sizes obtained from H_2 chemisorption data on catalysts prepared from $RuCl_3 \cdot 1.5H_2O$ are 79.3 Å for treatment II and 148.7 Å for treatment I. The difference between sizes is 22% for the Cl^- free catalyst and 90% for the Cl-containing one. Therefore, although the oxidation step could induce some Ru sintering, there must be another effect to account for the observed difference. It could be, as we already mentioned, the presence of residual chlorine.

We believe the TPR profiles support previous conclusions. The oxidation treatment at high temperature produces species that are more difficult to reduce in the temperature range we used. The signal belonging to the reduction of Ru is shifted toward higher temperatures. Similar shifts in TPR-experiments were reported by Berbé *et al.* (*46*). In previous work done in this laboratory on Ru/SiO_2 catalyst prepared from nitrates, the Ru reduction peak in the TPR profile appeared always at about the same temperature regardless the oxidation treatment (*15*). Therefore, we associated these temperature shifts in the Ru reduction peak with the treatment to the presence of residues of the $RuCl_3$ used in the preparation of the catalyst.

Comparing the TPD and TPSR profiles of 100 RuMo pretreated according to procedure I and II, it is evident that the area under the peaks is smaller for the catalyst subjected to I. Since similar amounts of catalysts and operating conditions were used in both cases, the observation is related to a smaller volume of desorbing gases. Reasoning in a similar way than in previous experiments, the observed effect is interpreted as the result of the partial blockage of the adsorbing surface by the residual chlorine. Obviously in this modified adsorption sites, elimination of weakly adsorbed species occurs during steps previous to temperature programming.

We conclude that the decrease in H_2 uptake in the chemisorption experiments after treatment I is mainly due to causes (i) and (ii) listed above, although the presence of oxidized Ru hard to reduce to Ru^0 is not discarded.

We turn our attention now to the presence of the second metal. When Mo is incorporated in the catalysts, a drop in H_2 and CO chemisorption is observed regardless the pretreatment. Let us consider treatment II first. For bimetallic catalysts exposed to that treatment (free of Cl) the addition of Mo produces a 60% decrease in hydrogen chemisorption referred to the pure Ru catalysts. The TPR profiles of those catalysts indicate an Ru–Mo interaction. It is evident by not only a smaller H_2 chemisorption than in the case of the pure Ru catalyst, but also a shift of the Ru reduction peak toward higher temperatures. Similar effects were previously reported for the Ru–Fe system (*26, 47*). Since equal amounts of catalysts were used in the experiments, which contains the same amount of Ru, the decrease in H_2 consumption by the 50 RuMo catalyst during the TPR, compared to that of 100 RuMo, is an indication that part of the Ru particles are

totally covered by the relatively large crystallites of an MoO_x species that blocks the access of the reducing gas, while the rest of the Ru particles are completely or partially free of MoO_x.

Considering treatment I, Table 3 shows the mean particle diameters of metal particles of 50 RuMo catalysts after this treatment, calculated from chemisorption data and from XRD data. There is an order of magnitude difference between them (1089.3 and 130.4). This cannot be attributed to experimental error and the only possible explanation is the partial blockage of adsorption sites.

Chlorine elimination during treatment I is similar for both the pure Ru and the bimetallic. Therefore, the presence of residual Cl could explain one-half of the drop in H_2 chemisorption in the 50 RuMo sample with respect to that of 100 RuMo (approximately this percentage drop is observed for 100 RuMo catalyst treated according to I with respect to the sample treated following II). Therefore the rest of the chemisorption decrease in 50 RuMo after I compared to 100 RuMo after I is due to the presence of Mo. This means that regardless the presence of some poisons on the surface, Mo covers the Ru particles to some extent preventing H_2 adsorption.

In the series treated with procedure I, the amount of H_2 consumed during the TPR of 100 RuMo and 50 RuMo is similar (see Table 2). It has been already mentioned that treatment I produces larger Ru particles. Therefore, although an Ru–MoO_x contact is probable, the complete coverage of the Ru particles is not possible. Nevertheless, as already mentioned, XRD results indicate the existence of Ru^0 and MoO_2 in the bimetallic catalyst after treatment I.

Results similar to those here described were reported by Van der Berg *et al.* (*28*). In order to explain the decrease in H_2 uptake and the shift to higher temperatures of the TPR peak of the main metal upon addition of the promoter in their Rh–Mo–Mn/SiO_2 catalysts, they postulated that an oxide of the promoter was partially covering the Rh particles. At this point it is interesting to recall that in alloys surface enrichment corresponds to the component having the lowest surface energy. In bimetallic catalysts, this is so unless a support interaction masks the normal enrichment effect (*48*).

On the other hand, it is known that the SMSI effect on Rh/TiO_2 results in a partial coverage of the metal by TiO_{2-x} during high-temperature reductions. This was explained in terms of a lower surface energy of TiO_2 and a favorable Rh–Ti interaction (*49*). In the present case, the decrease in H_2 uptake is not the result of the metal coverage either by the support or by a second metal but the coverage of Ru by an oxide incorporated as a promoter, formed during the pretreatment. The driving force for this Ru coverage by Mo oxide is the large difference between their free surface energy and the weak Mo–SiO_2 interaction, as is widely recognized (*50*). The following data are relevant to this discussion.

The heat of vaporization of Ru is 148 kcal/atg, while that of MoO_3 is 33 kcal/gmol. Besides, the vapor pressure of MoO_3 at temperatures close to 673 K is more or less 1 mmHg, while for bulk Ru a vapor pressure this high is reached around 2300 K (*51*).

The melting point of MoO_3 is 1068 K, that means that at the temperature of our treatments it is mobile. The free surface energies of Ru and MoO_3 are 3409 erg/cm^2 and 50–70 erg/cm^2, respectively (*52, 53*).

Another fact that favors the model of Ru particle covered by MoO_x occurs during the catalyst preparation procedure. Since the UV spectra indicated that there was no Ru–Mo interaction in the solution containing the precursors, we believe that it is in the support impregnation step where such interaction actually begins.

During impregnation, the pH of the solution contacting the SiO_2 is about 4, which is well above the isoelectric point of the support. Therefore, the support should tend to adsorb cations like Ru^{3+}, $[RuCl_2]^+$, or $RuCl^{2+}$ (*54*). On the other hand, Mo, that is

supplied by the $Mo_7O_{24}^{6-}$ anion (*55, 56*) should be repelled by the support as long as it remains wet, and it could seek positively charged sites close to Ru cations already in the surface. In such a way, although the procedure used was not an equilibrium impregnation, during the water evaporation process, Mo could be close to Ru. The subsequent steps in the treatment originates the species that finally covers the Ru particle.

Ammonium heptamolybdate decomposes thermally following the sequence (*57*)

$$(NH_4)6Mo_7O_{24} \cdot 2H_2O \xrightarrow{(463\ K)} 2(NH_4)_2O \cdot 5MoO_3 \xrightarrow{(518\ K)} (NH_4)_2O \cdot 8MoO_3 \xrightarrow{(633\ K)} MoO_3.$$

The heat involved in the decomposition of 1 mole of MoO_2 or MoO_3 is 140.6 and 65 kcal, respectively. The latter is obviously more easily decomposed. This fact favor the formation of channels through which H_2 reaches the Ru particles. The pretreatment defines the characteristics of this oxide layer.

When treatment II is used, the Mo precursor (Mo^{6+}) would decompose in H_2 atmosphere, originating a thin layer of MoO_2 (not detectable by XRD), that eventually totally covers about half of the total Ru particles present. Uncovered Ru particles remain unmodified as we found conducting ethane hydrogenolysis studies. These studies were performed on 100 RuMo and 50 RuMo pretreated following procedure II. The turnover frequency based on the Ru surface atoms determined from the chemisorption results cited herein are similar for both catalysts, with no change in the activation energy.

If treatment I is used, the oxidation step would originate the formation of MoO_3 leaving open places, which facilitates the H_2 access to the oxidized Ru particles. The Mo oxide layer is reduced to a larger extent than in the case of treatment II, therefore, CO and H_2 chemisorption on Mo is also possible.

Let us discuss now the results corresponding to pure molybdenum catalysts. The TPR profiles of the 0 RuMo samples indicate that six times more H_2 is consumed in the reduction of the Mo oxide after treatment II than after treatment I. This fact is consistent with the presence of CO and CH_4 in the TPSR profiles of 0 RuMo after treatment II. It also agrees with the difference in catalytic activity observed for 0 RuMo after each pretreatment. XPS spectra of the pure Mo catalysts, though showing the existence of different oxidation states of Mo (from 3^+ to 6^+) after both treatments, indicate that the number of reduced species is more important in 0 RuMo after treatment II.

Considering the activity for the syngas reaction, the presence of Cl in metallic catalyst is generally regarded as detrimental (*35*). However, its promotional effect on Mo/SiO_2 catalyst for the synthesis of oxygenates from CO and H_2 has been recently postulated (*58*). The effect of Cl on the vibration frequency of adsorbed CO is a shift of this frequency toward a higher wavenumber. This is indicative of a stronger C–O bond. As a result of it, dissociation is more difficult (*59*). We believe this is the reason for the lower activity shown by Ru catalysts after treatment I relative to the activity of those treated according to II.

Lu and Tatarchuk (*42*) mentioned that a lower electronic density in Ru is possible if Cl is present. Ionic species have been regarded as necessary for the production of oxygenates from CO and H_2 (*60*). In the case of 100 RuMo treated according to procedure I, this could favor a moderate change of selectivity to methanol.

In the case of the bimetallics, the activity results are in accordance with the hypothe-

sis of the partial coverage of the Ru particles by MoO_x. The better oxygenates and higher hydrocarbon selectivity observed during the activity tests of the catalysts treated according to I are consistent with this model. Similar results were reported by Takahashi *et al.* (*19*) and Mori *et al.* (*25*). Molybdenum has also been reported as active for oxygenates synthesis (*61–64*). This was associated with its valence and the existence of an Mo–support interaction (*65, 66*).

In the case of 0 RuMo catalysts, no significant differences were detected in the selectivity of differently treated samples. This result would indicate that the surface of 0 RuMo is qualitatively similar after both treatments, despite the differences noted in the XPS spectra and in H_2 chemisorption.

CONCLUSIONS

CO-impregnation of SiO_2 with $RuCl_3 \cdot 1 \cdot 5H_2O$ and ammonium heptamolybdate leads to a catalytic material in which Ru and Mo are in contact.

The presence of residual chlorine in the catalysts depends on the pretreatment used and produces changes in selectivity.

Molybdenum oxide species tend to cover Ru particles. The Ru–Mo contact seems to play a role in CO hydrogenation to oxygenates. The production of these Ru–Mo contacts depends on the size of Ru crystallites (which in turn depends on the pretreatment used) and the relative amounts of Ru–Mo present on the catalysts' support.

REFERENCES

1. Klier, K., *in* "Catalysis of Organic Reactions" (W. R. Moser, Ed.). Dekker, New York, 1981.
2. Natta, G., Colombo, U., Pasquon, I., and Emmet, P. H., (Eds.), "Catalysis," Vol. V, 131. Reinhold, New York, 1957.
3. Sugier, A., and Freund, E., U.S. Patent 4,122,110 (1978).
4. Schulz, J. F., Karn, F. S., and Anderson, R. E., Report 6974. U.S. Bureau of Mines, Washington, DC, 1967.
5. Kellner, C. S., and Bell, A. T., *J. Catal.* **71,** 288, (1981).
6. Bossi, A., Garbassi, F., and Petrini, G., *J. Chem. Soc. Faraday Trans.*, 1 (1982).
7. Kobori, Y., Yamasaki, H., Naito, S., Onishi, T., and Tamaru, K., *Chem. Lett.*, 553 (1983).
8. Knifton, J. F., *J. Chem. Soc. Chem. Commun.*, 729 (1983).
9. Knifton, J. F., *Organometallics* **3,** 62 (1984).
10. Hamada, H., Kiwahara, Y., Kintaichi, Y., Ito, T., Wakabayashi, Hijima, H., and Sano, K., *Chem. Lett.*, 1611 (1984).
11. Inoue, M., Miyake, T., Inui, T., and Takegami, Y., *J. Chem. Soc. Chem. Commun.*, 70, (1983).
12. Inoue, M., Miyake, T., Inui, T., and Takegami, Y., *Appl. Catal.* **11,** 103 (1983).
13. Inoue, M., Miyake, T., Inui, T., and Takegami, Y., *Appl. Catal.* **29,** 285 (1987).
14. Robertson, S. D., Mc Nicol, B. D., de Bass, J. H., Kluet, S. C., and Jenkins, J. W., *J. Catal.* **37,** 424 (1975).
15. Damiani, D. E., Perez Millán, E. D., and Rouco, A. J., *J. Catal.* **101,** 162 (1986).
16. Gorte, R. J., *J. Catal.* **75,** 164, (1982).
17. Rieck, J. S., and Bell, A. T., *J. Catal.* **85,** 143, (1984).
18. Dalla Betta, R. A., *J. Catal.* **34,** 57, (1974).
19. Takahashi, N., Mori, T., Miyamoto, A., Hattori, T., and Murakami, Y., *App. Catal.* **38,** 301, (1988).
20. Kip, B. J., Hermans, E. G. F., van Wolput, J. H. M. C., Hermans, N. M. A., van Grondelle, J., and Prins, R., *Appl. Catal.* **35,** 109, (1987).
21. Bhore, N. A., Bischoff, K. B., Manogue, W. H., and Mills, G. A., *in* "New Catalytic Materials in Fuels Processing." American Chemical Society Symposium Series, ACS, Washington, DC, 1990.
22. Mills, G. A., *in* "Division of Fuel Chemistry, American Chemical Society, Boston Meeting, April, 1990." ACS, Washington, DC, 1990.
23. Hicks, R. F., Yen, Q., and Bell, A. T., *J. Catal.* **89,** 498 (1984).
24. Inoue, M., Miyake, T., Inui, T., and Takegami, Y., *Appl. Catal.* **29,** 285 (1987).
25. Mori, M., Miyamoto, A., Takahashi, N., Fukagaya, M., and Murakami, T., *J. Phys. Chem.* **90,** 5197, (1986).
26. Stoop, F., and van der Wiele, K., *Appl. Catal.* **23,** 35 (1986).
27. Rouco, A. J., Haller, G. L., Oliver, J. A., and Kemball, C., *J. Catal.* **84,** 297 (1983).
28. Van der Berg, F. G. A., Glezer, J. H. E., and Sachtler, W. M. H., *J. Catal.* **93,** 340 (1985).
29. Rodríguez Cárdenas, H. E., Ph.D. Thesis, Universidad Nacional del Sur, 1989.
30. Miura, H., Osaka, M., Sugiyama, K., and Matsuda, T., *J. Catal.* **101,** 178 (1986).
31. Bond, A., Rajaram, F., and Burch, R., *Appl. Catal.* **27,** 379, (1986).
32. Koopman, P. G. J., Kieboom, A. P. G., and van Bekkum, H., *J. Catal.* **69,** 172 (1982).
33. Bossi, A., Garbassi, F., Orlandi, A., Petrini, G., and Zanderighi, L., "Studies in Surface Science

and Catalysis," Vol. 3, p. 405. Elsevier, Amsterdam New York, 1979.
34. Blanchard, G., Charcosset, H., Chenebauz, M. T., and Primet, M., "Studies in Surface Science and Catalysis," Vol. 3, p. 197. Elsevier, Amsterdam New York, 1979.
35. Mieth, J. A., and Schwarz, J. A., *J. Catal.* **118,** 218, (1989).
36. Ono, T., Anpo, M., and Kubokawa, Y., *J. Phys. Chem.* **90,** 4780 (1986).
37. Narita, T., Miura, H., Sugiyama, K., Matsuda, T., and González, R. D., *J. Catal.* **103,** 492 (1987).
38. Low, G. G., and Bell, A. T., *J. Catal.* **57,** 397, (1979).
39. Don, J. A., Pijpers, A. P., and Scholten, J. J. F., *J. Catal.* **80,** 296 (1983).
40. Davidov, A. A., and Bell, A. T., *J. Catal.* **49,** 332 (1977).
41. Mukherji, R., Ph.D. Thesis, Univ. of Rhode Island, 1977.
42. Lu, K., and Tatarchuk, B. J., *J. Catal.* **106,** 166 (1987).
43. Lu, K., and Tatarchuk, B. J., *J. Catal.* **106,** 176 (1987).
44. Stoop, F., Verbiest, A. M. G., and van der Wiele, K., *Appl. Catal.* **25,** 51 (1986).
45. Anderson, J. R., "Structure of Metallic Catalysts." Academic Press, New York, 1975.
46. Berbé, R., Bossi, A., Garbassi, F., and Petrini, G., *in* "Proceedings of the VII International Conference on Thermal analysis" (B. Miller, Ed.), Vol. II, p. 1224. Wiley, New York, 1982.
47. Guczi, L., Schay, Z., Matusek, K., and Bogyay, I., *Appl. Catal.* **22,** 289 (1986).
48. Sinfelt, J. H., *J. Catal.* **29,** 308 (1973).
49. Haller, G. L., Sakellson, S., and Mc Millan, M., *J. Phys. Chem.* **90,** 1733, (1986).
50. Gajardo, P., Declerck-Grimwe, R. I., Delvaux, G., Olodo, P., Zabala, J. M., Canesson, P., Grange, P., and Delmon, B., *in* "Proceedings of the Climax Second International Conference on the Chemistry and Uses of Molibdenum" (P. C. H. Mitchell, Ed.), p. 150. Climax Molibdenum Co., London, 1977.
51. Weast, R. G., *in* "Handbook of Chemistry and Physics" (R. G. Weast and S. M. Selz, Eds.). The Rubber Chemical Co., Cleveland, 1967.
52. Overbury, S. H., Bertrand, P. A., and Somorjai, G. A., *Chem. Rev.* **75**(5), 547 (1975).
53. Mezey, L. Z., and Giber, J., *Japn. J. Appl. Phys.* **21**(11), 1569 (1982).
54. Connick, R. E., and Fine, D. E., *J. Am. Chem. Soc.* **82,** 4187 (1960).
55. Aveston, J., Wanacker, E., and Johnston, J. S., *Inorg. Chem.* **3,** 735 (1964).
56. Lerf, A., Vogdt, C., Butz, T., Eid, A. M. M., and Knozinger, H., *Hyperfine Interact.* **15/16,** 921 (1983).
57. Hanafi, Z. M., Khilla, M. A., and Askar, M. H., *Thermochim. Acta* **45,** 221 (1981).
58. Tatsumi, T., Muramatsu, A., Yokota, K., and Tominaga, H., *in* "Methane Conversion" (D. M. Bibby, C. D. Chang, R. F. Howe, and Yurrchak, Eds.), p. 219. Elsevier, Amsterdam, 1988.
59. Chen, H. W., Zhong, Z., and White, J. M., *J. Catal.* **90,** 119 (1984).
60. Driessen, J., Poels, E. K., Hindermann, J. P., and Ponec, V., *J. Catal.* **82,** 261 (1983).
61. Tatsumi, T., Muramatsu, A., and Tominaga, H., *Chem. Lett.*, 685 (1984).
62. Tatsumi, T., Muramatsu, A., Tominaga, H., and Fukunaga, T., *Polyhedron* **5,** 257 (1985).
63. Tatsumi, T., Muramatsu, A., and Tominaga, H., *Appl. Catal.* **27,** 69 (1986).
64. Dun, J. W., Gulari, E., and Ng, K. Y. S., *Appl. Catal.* **15,** 247 (1985).
65. Concha, B. E., and Bartholomew, C. H., *J. Catal.* **79,** 327 (1983).
66. Muralidhar, G., Concha, B. E., Bartholomew, G. L., and Bartholomew, C. H., *J. Catal.* **89,** 274 (1984).